Internal Signal Stochastic Resonance in a Modified Flow Oregonator Model Driven by Colored Noise

Shi Zhong[†] **and Houwen Xin***[,†,‡]

Department of Chemical Physics, University of Science and Technology of China, Hefei, Anhui, 230026, P.R. China, and National Laboratory of Theoretical and Computational Chemistry of China, Jilin, Changchun, 130023, P.R. China

Received: July 13, 1999; In Final Form: October 11, 1999

In the majority of studies on stochastic resonance, white noise without any time correlation has been used. In this paper, a modified Oregonator-type model, which was proposed to account for the photosensitivity of the $R_u(bpy)_3^{2+}$ catalyzed Belousov−Zhabotinsky reaction in a flow system, is investigated when the control parameter, light flux, is modulated by colored noise near a Hopf bifurcation point. Noise induced coherent oscillations (NICO) are observed, and the signal-to-noise ratio (SNR) goes through a maximum with the increment of noise intensity indicating occurrence of internal signal stochastic resonance (ISSR). In addition, the SNR also shows resonance behavior with the variation of correlation time of colored noise. The aspects of the ISSR in this system are discussed.

I. Introduction

Noise is typically thought of as the enemy of order rather than as a constructive influence. It makes clear signals or patterns obscure, and it also makes the detection of weak signal impossible. However, recent research has show that in nonlinear systems, the presence of noise can affect the time evolution of a system in a counterintuitive way via a mechanism known as stochastic resonance (SR). The concept of SR was originally put forward by Benzi and his collabrators to account for the periodic oscillations of the earth's ice ages.[1] The first experimental verification was obtained by Fauve and Heslot in a noise-driven electronic circuit known as the Schmitt trigger.[2] In the past decades the counterintuitive phenomena of SR have been extensively studied.[3] At present time more and more scientists, whose majors vary from biology, physics to chemistry,[4,5] have paid considerable attention to these surprising phenomena, that noise with suitable intensity can increase the detectability of weak input signal in a nonlinear system and that the signal-to-noise ratio (SNR) goes through a maximum with the increment of noise intensity. Recent theoretical research has proved that SR can occur under many situations. For instance, the system can be monostable,[6] excitable,[7] threshold-free,[8] or spatial-extended;[9] the signal can be periodic, aperiodic, or chaotic;[10] the noise can be white or colored,[11] furthermore the noise can be internal[11,12] or external[4,5] for a system.

Recently, it is reported that the external signal can be replaced by "internal signal", such as periodic oscillations in a deterministic system.[13] When the control parameter is modulated by random force near the bifurcation point between a stable node and a limit cycle, noise induced coherent oscillations (NICO) are observed, and the SNR goes through a maximum with the increment of noise intensity. We called this type of SR internal signal stochastic resonance (ISSR).[14] In this paper we adopted a newly developed Oregonator[15]-type model, which was proposed by Amemiya et al.[16] to account for the photosensitivity[17,18] of the BZ[19] reaction in a flow system, to investigate the ISSR behavior. When the control parameter, light flux, is modulated by colored noise near a Hopf bifurcation point, noise induced coherent oscillations were observed and the SNR went through a maximum indicating the occurrence of ISSR. Furthermore, the system also showed resonance behavior with the variation of correlation time of the colored noise.

II. Model

A. Photosensitive Flow-Oregonator. A modified Oregonator model, which has been proposed by Kádár and co-workers,[17] accounting for the photosensitivity of the BZ reaction in a flow system involves the following reaction steps:

$$A + Y \rightarrow P + X \tag{O1}$$

$$X + Y \rightarrow 2P \tag{O2}$$

$$A + X \rightarrow 2X + 2Z \tag{O3}$$

$$2X \rightarrow P + A \tag{O4}$$

$$M + Z \rightarrow hY \tag{O5}$$

$$G \leftrightarrows E \tag{PO}$$

$$E + V \rightarrow Y + Z \tag{P1}$$

$$E + A \rightarrow X + 2Z \tag{P2}$$

where $A = B_rO_3^-$, $P = HOB_r$, $X = HB_rO_2$, $Y = B_r^-$, $Z = Ru(bpy)_3^{3+}$, M = MA (malonicacid), $G = Ru(bpy)_3^{2+}$, $E = Ru(bpy)_3^{2+*}$(excited state of $Ru(bpy)_3^{2+}$), $V = B_rMA$, and h is the stoichiometric factor. Processes O1−O5 represent the Oregonator, while processes PO−P2 represent the photochemical reaction of the catalyst; PO is the photoactivation of $Ru(bpy)_3^{2+}$ with the forward reaction rate proportional to the light flux (Φ), and the reverse reaction is a first-order quenching

* To whom correspondence should be addressed.
† University of Science and Technology of China.
‡ National Laboratory of Theoretical and Computational Chemistry of China.

10.1021/jp9923466 CCC: $19.00
Published on Web 12/22/1999

TABLE 1: Parameters Used in the Model

parameters	ref
Rate Constants	
$K_{O1} = (2\ M^{-3}\ s^{-1})H^2$	22
$K_{O2} = (3 \times 10^6\ M^{-2}\ s^{-1})H$	22
$K_{O3} = (42\ M^{-2}\ s^{-1})H$	22
$K_{O4} = 3 \times 10^3\ M^{-1}\ s^{-1}$	22
$K_{O5} = 5\ M^{-1}\ s^{-1}$	16
Stoichiometric Factor and Concentrations	
$h = 0.5$	16
$H = 0.37$ M	16, 17
$A = 0.15$ M	16, 17
$M = 0.2$ M	16, 17
$V = 0.05$ M	16, 17
Initial Conditions	
$X_0 = 0$ M	16
$Y_0 = 0$ M	this paper
$Z_0 = 0$ M	16
$K_f = 2.2 \times 10^{-3}\ s^{-1}$	this paper

process with a rate constant of k_{-po}. P1 and P2 represent the photoinduced generation of HB_rO_2, B_r^-, and $Ru(bpy)_3^{3+}$ from the reaction of $Ru(bpy)_3^{2+*}$ with B_rMA and $B_rO_3^-$. The flow terms are added to the differential rate equations as

$$\frac{dX}{dt} = K_{O1}AY - K_{O2}XY + K_{O3}AX - 2K_{O4}X^2 + P_2\Phi - k_f X$$
$$\frac{dY}{dt} = -K_{O1}AY - K_{O2}XY + hK_{O5}MZ + P_1\Phi - k_f Y$$
$$\frac{dZ}{dt} = 2K_{O3}AX - K_{O5}MZ + P_1\Phi + 2P_2\Phi - k_f Z \quad (1)$$

where $P_1\Phi$ and $P_2\Phi$ are the reaction rates for processes P1 and P2, k_f is the flow rate, and A, M, and V are constants in this flow system. By using the Tyson's scaling,[20] the dimensionless rate equations then become

$$\epsilon \frac{dx}{d\tau} = x(1-x) + y(q-x) - \epsilon K_f x + p_2\phi$$
$$\epsilon' \frac{dy}{d\tau} = 2hz - y(q+x) - \epsilon' K_f y + p_1\phi$$
$$\frac{dz}{d\tau} = x - z - K_f z + \left(\frac{P_1}{2} + p_2\right)\phi \quad (2)$$

where

$$x = \frac{2k_{O4}}{k_{O3}A}X \qquad y = \frac{k_{O2}}{k_{O3}A}Y \qquad z = \frac{k_{O4}k_{O5}M}{(k_{O3}A)^2}Z \qquad \tau = k_{O5}\,Mt$$
$$y_0 = \frac{k_{O2}}{k_{O3}A}Y_0,\ K_f = \frac{1}{k_{O5}M}k_f$$
$$\phi = \frac{2k_{O4}}{(k_{O3}A)^2}\Phi \qquad \epsilon = \frac{k_{O5}M}{k_{O3}A} \qquad \epsilon' = \frac{2k_{O4}k_{O5}M}{k_{O2}k_{O3}A}$$
$$q = \frac{2k_{O1}k_{O4}}{k_{O2}k_{O3}}$$
$$p_1 = \frac{V}{0.089 + V + 15H^2A} \qquad p_2 = \frac{15H^2A}{0.089 + V + 15H^2A}$$

For details see refs 16, 20−22. The rate constants and other parameters used in this model are listed in Table 1. The initial concentration of B_rMA affects the dynamics of this system.[17] In this paper we adopted a high value of B_rMA concentration to investigate how colored noise affects the dynamics of this system near a Hopf bifurcation point.

B. Random Modulation of Light Flux. The light flux is composed of a constant and a random component. It can be expressed as follows:

$$\Phi = \Phi_0[1 + \beta\xi(t)] \quad (3)$$

where Φ_0 is the constant component, β is intensity of the colored noise $\xi(t)$. We can introduce another equation as follows:

$$\frac{d\xi(t)}{dt} = -\frac{1}{\tau_0}\xi(t) + \Gamma(t) \quad (4)$$

where $\Gamma(t)$ is Gaussian distributed white noise with zero mean value $\langle\Gamma(t)\rangle = 0$ and autocorrelation function $\langle\Gamma(t)\Gamma(t')\rangle = 2D\delta(t - t')$; 2D is variance. Equation 4 is a Langevin equation (LE). The mean value of variable $\xi(t)$ is

$$\langle\xi(t)\rangle = \langle\xi(0)\rangle \exp(-t/\tau_0) \quad (5)$$

and the autocorrelation function of it is

$$\langle\xi(t)\,\xi(t')\rangle = D\tau_0 \exp(-|t - t'|/\tau_0) \quad (t/\tau_0,\ t'/\tau_0 \gg 1) \quad (6)$$

where $\langle\xi(0)\rangle$ is statistical mean value of random variable at initial time. So $\xi(t)$ is exponential Gaussian colored noise, and τ_0 is the correlation time of it. Its power spectra have Lorentzian distribution: $S(\omega) = \int \exp(-i\omega\tau)D\tau_0 \exp(-|\tau|/\tau_0)d\tau = 2D\tau_0^2/(1 + \tau_0^2\omega^2)$. Therefore, by enlarging the dimensions of eq 2, we can investigate the effects of colored noise on the dynamics of this system. The constant component was chosen in such a way that the system remained in the steady state without the modulation of noise. The system was modulated in the following two ways to show ISSR: (i) varying noise intensity with constant correlation time; (ii) varying correlation time with constant noise intensity. We chose three correlation times $\tau_0 =$ 1s, 2s, 10s, and three noise intensities $\beta = 0.1, 0.2, 0.3$ to study this system, respectively. The noise pulse length [4] and variance ($2D$) of $\Gamma(t)$ were set as 0.2 s and 1, respectively, in this paper. Equations 2−4 with the values of the parameters listed in Table 1 were integrated numerically by using the fourth-order Runge−Kutta method ($dt = 0.01$ s, total time 60000 s, total number of data 60000).To quantify the ISSR effect, the time series of y (proportional to the concentration of B_r^-) were analyzed by the Fourier spectra.

III. Results

A linear stability analysis for this three-variable system with $\beta = 0$ was carried out. The bifurcation diagram is show in Figure 1. A subcritical Hopf bifurcation occurs at $\Phi_0 \approx 1.623 \times 10^{-6}$ Ms^{-1}; undamped large-amplitude oscillations (spikes) stopped or started abruptly when the value of the light flux was increased or decreased gradually. The dotted line indicates the amplitude of oscillations in y (proportional to B_r^-). We chose $\Phi_0 = 1.63 \times 10^{-6}$ Ms^{-1}, which is close to the bifurcation point for ISSR study.

A. Varying Noise Intensity with Constant Correlation Time. Figure 2 shows the results as a function of noise intensity with correlation time $\tau_0 = 1$ s. Without noise, the system exhibited no response (Figure 2a). Irregular spikes occurred at noise intensity $\beta \approx 0.06$ (Figure 2b). When the noise intensity

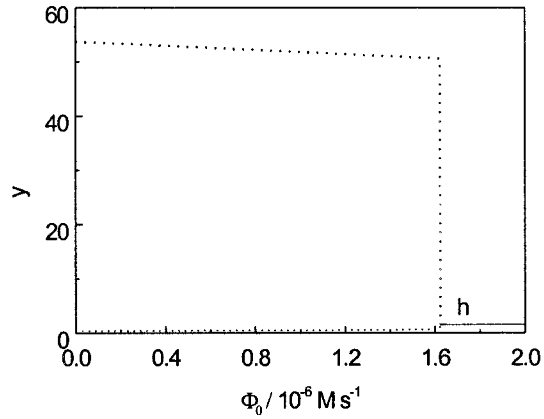

Figure 1. The bifurcation diagram of the modified Oregonator model (eqs 2−4 with $\beta = 0$). The other parameters used are listed in Table 1. The dotted line indicates amplitude of oscillations in *y* (proportional to the concentration of B_r^-). A subcritical Hopf bifurcation occurs at $\Phi_0 \approx 1.623 \times 10^{-6}$ Ms^{-1}. Here, h denotes the Hopf bifurcation point.

was increased, more orderly spikes appeared at $\beta \approx 0.44$ (Figure 2c), which resulted in a peak in the SNR to the noise level (Figure 3(i)a). If the noise intensity was further increased, the system generated more spikes with the period of the intrinsic oscillation (Figure 2d), which resulted in the decrease in the SNR. The above phenomena indicate the occurrence of ISSR. When longer correlation times were chosen, the maximum effect of ISSR is shifted to lower noise intensity: $\tau_0 = 2$ s, $\beta \approx 0.27$ (Figure 3(i)b); $\tau_0 = 10$ s, $\beta \approx 0.118$ (Figure 3(i)c). In Figure 3(i) the maximum of SNR also decreased with increasing correlation time of the colored noise.

B. Varying Correlation Time with Constant Noise Intensity. The system also shows resonance behavior with the variation of correlation time. The SNR reached its maximum at $\tau_0 \approx 4.06$ s with $\beta = 0.1$ (Figure 3(ii)a); the maximum effect of ISSR shifted to lower correlation time at $\tau_0 \approx 2.23$s with $\beta = 0.2$, 0.3 (Figure 3(ii)b and Figure 3(ii)c). It seems that τ_0 plays the same role as the noise intensity.

IV. Discussion

Generally speaking, the occurrence of NICO near the Hopf bifurcation point is not surprising, since the system enters the oscillatory region now and then by the noise perturbing the control parameter, which results in a peak in the Fourier spectra. With the increment of the noise intensity, the SNR goes through a maximum, indicating the occurrence of ISSR. As to our knowledge, in the majority studies on SR, white noise without any correlation time was used, especially in chemical reaction systems. In the present work we investigated the ISSR behavior near a Hopf bifurcation point in a photosensitive BZ reation driven by colored noise. A similar situation has been measured experimentally by Schneider and Münster[23] who observed optimal noise effects when the applied noise had a frequency which was close to the resonance frequency of the focus. What interests us most is that the correlation time of colored noise seems to play the same role as noise intensity for the occurrence of ISSR, and the largest SNR goes down as the color of the noise increases. The similar phenomenon has been reported by Hanggi et al.[24] White noise is Markovian noise, which describes short-time behavior, while colored noise (exponentially correlated) refers to the long-time dynamics of fluctuation which is a non-Markovian process. The time scale of the two noises

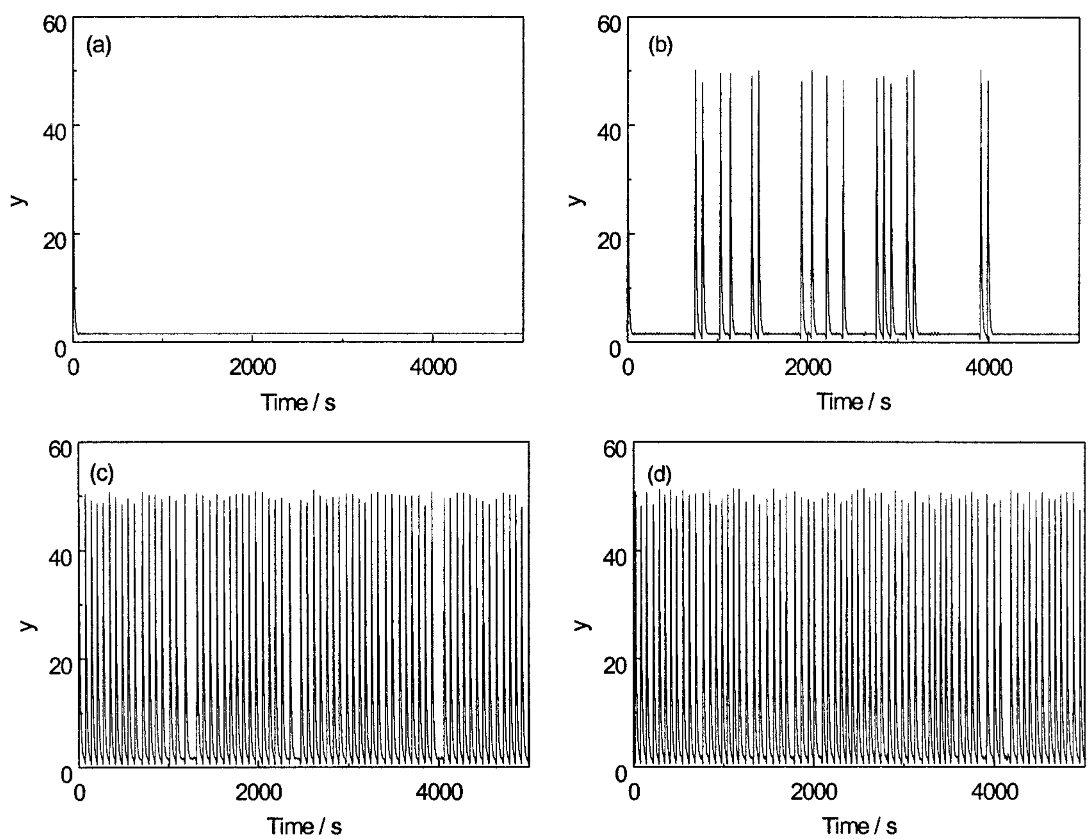

Figure 2. Oscillations in *y* as a function of the intensity of the colored noise with noise crrelation time $\tau_0 = 1$ s and noise pulse length $\tau = 0.2$ s. $\beta = 0$ (a); $\beta = 0.06$ (b); $\beta = 0.44$ (c); $\beta = 0.92$ (d). A total of 60000 points were recorded at the intervals 1 s, and the result up to 5000 s is shown. The parameters used are the same as those in Figure 1.

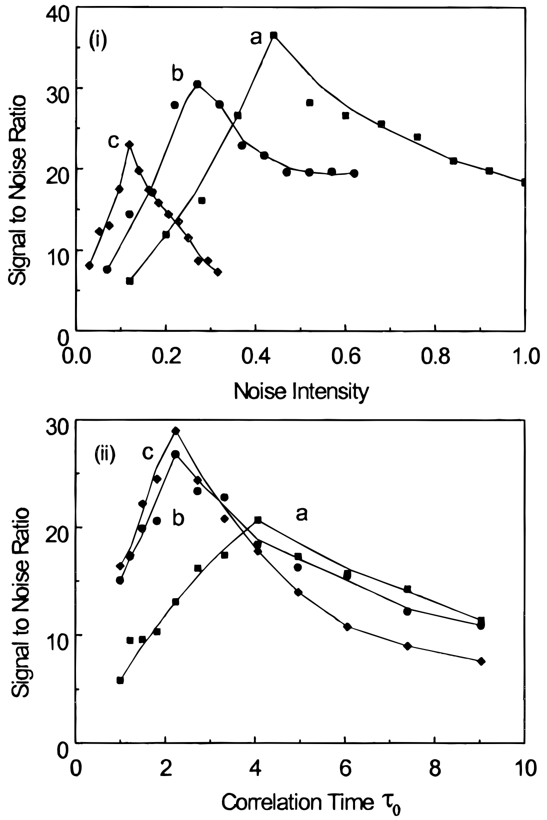

Figure 3. Internal signal stochastic resonance (ISSR). (i) SNR as evaluated from the Fourier spectra versus noise intensity. The SNR passes through a maximum at $\beta \approx 0.44$ with $\tau_0 = 1$ s (a); $\beta \approx 0.27$ with $\tau_0 = 2$ s (b); $\beta \approx 0.118$ with $\tau_0 = 10$ s (c). (ii) SNR as evaluated from the Fourier spectra versus correlation time of colored noise. The maximum effect of ISSR occurs at $\tau_0 \approx 4.06$ s with $\beta = 0.1$ (a); $\tau_0 \approx 2.23$ s with $\beta = 0.2$, 0.3 (b) and (c). The solid lines are meant as guides to the eyes.

is different, which resulted in the difference in their effects on SR. In addition, a proper theoretical model would be of great help to the future research.

Acknowledgment. This work is supported by the National Science Foundation of China.

References and Notes

(1) Benzi, R.; Sutera, S.; Vulpiani, A. *J. Phys. A* **1981**, *14*, L453.

(2) Fauve, S.; Heslot, F. *Phys. Lett. A* **1983**, *97*, 5.

(3) For a review of stochastic resonance, see: Gammaitoni, L.; Jung, P.; Marchesoni, F. *Rev. Mod. Phys.* **1998**, *70*, 223. Wiesenfeld, K.; Moss, F. *Nature* **1995**, *373*, 33. Wiesenfeld, K.; Jaramillo, F. *Chaos* **1998**, *8*, 539.

(4) Guderian, A.; Dechert, G.; Zeyer, K. P.; Schneider, F. W. *J. Phys. Chem.* **1996**, *100*, 4437. Föster, A.; Merget, M.; Schneider, F. W. *J. Phys. Chem.* **1996**, *100*, 4442. Hohman, W.; Müller, J.; Schneider, F. W. *J. Phys. Chem.* **1996**, *100*, 5388.

(5) Yang, L. F.; Hou, Z. H.; Xin, H. W. *J. Chem. Phys.* **1998**, *109*, 2002. Yang, L. F.; Hou, Z. H.; Xin, H. W. *J. Chem. Phys.* **1998**, *109*, 6456. Yang, L. F.; Hou, Z. H.; Xin, H. W. *J. Chem. Phys.* **1999**, *110*, 3591.

(6) Vilar, J. M. G.; Rubi, J. M. *Phys. Rev. Lett.* **1996**, *77*, 2863. Grigorenko, A. N.; Nikitin, S. I.; Roschepkin, G. V. *Phys. Rev. E* **1997**, *56*, R4097.

(7) Wiesenfeld, K.; Pierson, D.; Pantazelou, E.; Dames, C.; Moss, F. *Phys. Rev. Lett.* **1994**, *72*, 2125. Casado, J. M. *Phys. Lett. A* **1997**, *235*, 489. Collins, J. J.; Chow, C. C.; Imhoff, T. T. *Phys. Rev. E* **1995**, *52*, R3321. Eichwald, C.; Walleczek, J. *Phys. Rev. E* **1997**, *55*, R6315.

(8) Bezrukov, S. M.; Vodyanoy, I. *Nature* **1997**, *385*, 319. Jung, P.; Wiesenfeld, K. *Nature* **1997**, *385*, 291. Bezrukov, S. M.; Vodyanoy, I. *Chaos* **1998**, *8*, 557.

(9) Jung, P.; Mayer-Kress, G. *Phys. Rev. Lett.* **1995**, *74*, 2130. Horacio. S. W. *Phys. Rev. E* **1996**, *54*, R3075. Vilar, J. M. G.; Rubi, J. M. *Phys. Rev. Lett.* **1997**, *78*, 2886.

(10) Hu, G.; Gong, D. C.; Wen, X. D. *Phys. Rev. A* **1992**, *46*, 3250. Chow, C. C.; Imhoff, T. T.; Collins, J. J. *Chaos* **1998**, *8*, 616. Castro, R.; Sauer, T. *Phys. Rev. Lett.* **1997**, *79*, 1030.

(11) Neiman, A.; Sung, W. *Phys. Lett. A* **1996**, *223*, 341. Nozaki, D.; Yamamoto, Y. *Phys. Lett. A* **1998**, *243*, 281.

(12) Pikovsky, A. S.; Kurths, J. *Phys. Rev. Lett.* **1997**, *78*, 775.

(13) Hu, G.; Ditzinger, T.; Ning, C. Z.; Haken, H. *Phys. Rev. Lett.* **1993**, *71*, 807.

(14) Hou, Z. H.; Xin, H. W. *J. Chem. Phys.* **1999**, *111*, 721. Hou, Z. H.; Yang, L. F.; Xin, H. W. *J. Chem. Phys.* **1999**, *111*, 1592.

(15) Field, R. J.; Noyes, R. M. *J. Chem. Phys.* **1974**, *60*, 1877.

(16) Amemiya, T.; Ohmori, T.; Nakaiwa, M.; Yamaguchi, T. *J. Phys. Chem A* **1998**, *102*, 4357.

(17) Kádár, S.; Amemiya, T.; Showalter, K. *J. Phys. Chem A* **1997**, *101*, 8200.

(18) Yamaguchi, T.; Shimamoto, Y.; Amemiya, T. *Chem. Phys. Lett.* **1996**, *259*, 219. Kaminaga, A.; Hanazaki, I. *Chem. Phys. Lett.* **1997**, *278*, 16. Kaminaga, A.; Hanazaki, I. *J. Phys. Chem A* **1998**, *102*, 3307.

(19) Zaikin, A. N.; Zhabotinsky, A. M. *Nature* **1970**, *225*, 535. Field, R. J.; Koros, E.; Noyes, R. M. *J. Am. Chem. Soc.* **1972**, 94, 8649.

(20) Tyson, J. J. *Ann. N. Y. Acad. Sci.* **1979**, *316*, 279.

(21) Krug, H.-J.; Pohlmann, L.; Kuhnert, L. *J. Phys. Chem.* **1990**, *94*, 4862.

(22) Field, R. J.; Fösterling, H.-D. *J. Phys. Chem.* **1986**, *90*, 5400.

(23) Schneider, F. W.; Münster, A. F. *J. Phys. Chem.* **1991**, *95*, 2130.

(24) Hanggi, P.; Jung, P.; Zerbe, C.; Moss, F. *J. Stat. Phys.* **1993**, *70*, 25.